

Original Article



Effect of High Positive Acceleration (+Gz) Environment on Dental Implant Osseointegration: A Preliminary Animal Study*

ZHU Xiao Ru, DENG Tian Zheng, PANG Jian Liang, LIU Bing, and KE Jie[#]

Department of Stomatology, Air Force Medical Center, PLA, Beijing 100142, China

Abstract

Objective To observe the effect of high positive acceleration (+Gz) environment on dental implant osseointegration in a rabbit model and to investigate its mechanism.

Methods Forty-eight New Zealand white rabbits were randomly divided into 6 groups. The rabbit's mandibular incisors were extracted and 1 implant was placed in each socket immediately. After 1 week of rest, the rabbits were exposed to a high +Gz environment, 3 times a week. The rabbits were sacrificed at 3 weeks (2 weeks +Gz exposure), 5 weeks (4 weeks +Gz exposure), and 12 weeks (4 weeks +Gz exposure and 7 weeks normal environment) after surgery, respectively. Specimens were harvested for micro-CT scanning, histological analysis, and real-time polymerase chain reaction examination.

Results Compared with those in the control group, the mRNA expression levels of bone morphogenetic protein-2 (BMP-2), osteopontin (OPN), and transforming growth factor- β 1 (TGF- β 1) were significantly lower ($P < 0.05$), while the mRNA expression level of receptor activator of nuclear factor κ B ligand (RANKL) and the RANKL/osteoprotegerin (OPG) ratio were significantly higher ($P < 0.05$) at 3 weeks; values of bone volume fraction, trabecular number, bone-implant contact (BIC), and TGF- β 1 and OPG mRNA expression levels were significantly lower ($P < 0.05$), and the value of trabecular separation, RANKL mRNA expression level and RANKL/OPG ratio were significantly higher ($P < 0.05$) at 5 weeks; and the value of BIC was still significantly lower ($P < 0.05$) at 12 weeks in the experimental group.

Conclusion Early exposure to the high +Gz environment after implant surgery might have an adverse effect on osseointegration, and its mechanism could be related to the inhibition of osteoblast activity and promotion of osteoclast activity.

Key words: Positive acceleration; Osseointegration; Dental implant; Micro-CT; Real-time polymerase chain reaction; Osteoblast

Biomed Environ Sci, 2019; 32(9): 687-698 doi: 10.3967/bes2019.087

ISSN: 0895-3988

www.besjournal.com (full text)

CN: 11-2816/Q

Copyright ©2019 by China CDC

INTRODUCTION

C Pilots in an accelerating aircraft or spaceship are often exposed to the force of acceleration (hypergravity), especially the high sustained positive acceleration (+Gz) force acting along the body axis from head to toe. In some

extreme cases, pilots of modern high-performance fighter aircrafts have to suffer an acceleration as high as +9 Gz for 15 s to 45 s^[1,2]. Repeated exposure to high +Gz force can cause a series of physiological reactions in the body, including an increase in body weight and hydrostatic pressure, redistribution of blood to the lower body, and cerebral ischemia.

*This work was financially supported by China Postdoctoral Science Foundation [No. 2016M592971] and Logistics Department of the Chinese People's Liberation Army [No. AKJ15J003].

[#]Correspondence should be addressed to KE Jie, Professor, Tel: 86-10-66928052, E-mail: kejie630331@163.com

Biographical note of the first author: ZHU Xiao Ru, female, born in 1982, DDS, PhD, Attending Physician, majoring in stomatology.

These changes can damage the heart, brain, and nervous system^[3-5].

Fighter pilots who had undergone flight training in a high +Gz environment had increased bone mineral density in their cervical and thoracic vertebrae^[6,7]. Some studies have reported the effects of hypergravity on the load-bearing bone in different species. For example, animal studies in a 2 G hypergravity environment showed that the femur trabecular volume was increased in mice and the cortical bone was thickened^[8-10], but bone architectural changes were inconsistent in mice that lived in a 3 G hypergravity environment. Kawao et al. found that the mineral content of tibial trabecular bone in mice was increased in a 3 G hypergravity environment^[11]; while Gnyubkin et al. found that the cortical bone was thinned out, and bone formation rate was decreased in mice that lived in a 3 G hypergravity environment^[9]. The mechanisms that explain these changes are not clear yet, but we propose that a high hypergravity environment might have an adverse effect on bone formation.

It is believed that hypergravity environment can promote the differentiation of bone marrow mesenchymal stem cells into osteoblasts^[12-14], and influence the proliferation and differentiation of osteoblasts. From previous studies, we concluded that there might be a 'critical point' for the effects of hypergravity on osteoblasts and osseointegration. Below this 'critical point' hypergravity condition may promote osteoblast proliferation and inhibit differentiation^[15-18]. In contrast, above the 'critical point', the hypergravity condition may inhibit osteoblast proliferation and promote differentiation^[19-21].

In some countries, dental implant therapy has been applied in military pilots cautiously^[22]. Until now, there are little fundamental studies assessing the effect of high +Gz environment on osseointegration after tooth implant surgery. Therefore, the aims of our study are to observe the effect of high +Gz environment on dental implant osseointegration in a rabbit model and to investigate its mechanism.

MATERIALS AND METHODS

Implants Preparation

The screw-type titanium implants were manufactured by WeGo Group Co., Ltd (Yantai, Shandong, China). The implant size (3.0 mm in diameter and 12.0 mm in length) was specifically

designed to match the length and diameter of the rabbit mandibular incisors. The implant was a screw-type implant with micro threads and a smooth neck of 2 mm (Figure 1C). The implant surface was treated with sand-blasting with large grit and acid-etching (SLA) technology. Afterward, the implants were sterilized by gamma radiation and double packaged with a special design to ensure safe implant handling and placement, avoiding any hand contact.

Animal Surgery

Forty-eight adult, male New Zealand White rabbits (*Oryctolagus cuniculus*) weighing 2,485 (\pm 248) g were obtained from Beijing Vital River Laboratories. The animals were housed under appropriate environmental conditions, were exposed to 12-h light-dark cycles, and had access to standard food and water *ad libitum*. The protocol was approved by the Committee for Animal Experiments Ethics at the Air Force General Hospital, PLA, China (Protocol # kz2016006). All surgeries were performed under pentobarbital sodium anesthesia, and all necessary efforts to minimize animal discomfort were made.

The experimental scheme is illustrated in Figure 1A. The rabbits were randomly distributed into 6 equal groups (3 experimental groups and 3 control groups, 8 rabbits in each group). After one week of acclimation, the rabbits were anesthetized by an intraperitoneal injection of 3% pentobarbital sodium (1.2 mL/kg weight) (Sinopharm Chemical Reagent, Beijing, China) and were locally anesthetized with primacaine adrenaline (Produits Dentaires Pierre Rolland, Merignac, France). Bilateral mandibular incisors were extracted with minimal trauma to preserve the cortical bone. The implants were immediately placed into each tooth socket, and primary stability of the implants was achieved manually at about 15 N·cm. The gingiva was then closely sutured (Figure 1B, 1D). After surgery, all the rabbits had an intramuscular injection of penicillin (4×10^5 U/d) (North China Pharm, Shijiazhuang, Hebei, China) every day for 3 days.

+Gz Exposure

One week after surgery, the experimental rabbits were exposed to high +Gz environment 3 times a week for 2 or 4 weeks in an animal centrifuge, while the control rabbits were raised in a common environment. The rabbits in one experimental group were exposed to +Gz for 2 weeks, and then sacrificed along with those in a control group. The rabbits in the other two experimental groups were

exposed to +Gz for 4 weeks. Then the rabbits in one experimental group and one control group were killed at the end of 4 weeks. The rabbits in the 3rd experimental group were raised in a common

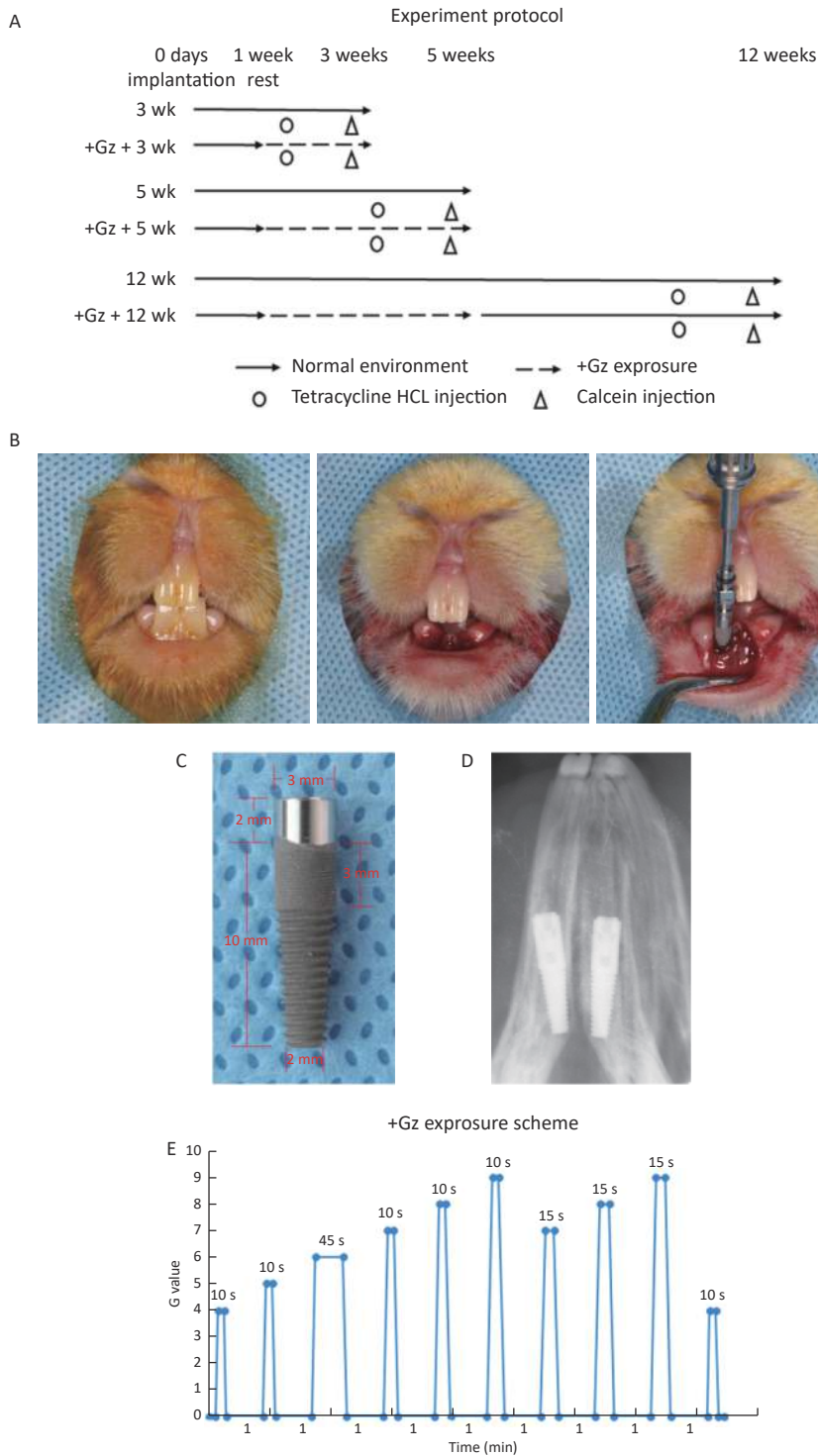


Figure 1. The effects of high +Gz environment on osseointegration after tooth implant surgery. (A) Experiment design and protocol. (B) Immediate implant placement surgery in rabbits. (C) View of the implant. (D) An X-ray film of the dental implant after immediate implantation. (E) The +Gz exposure protocol. wk, week.

environment for another 7 weeks after +Gz exposure, and then sacrificed along with those in the 3rd control group.

+Gz exposure was accomplished by using a specially designed animal centrifuge provided by the Air Force Aeromedicine Institute (Beijing, China). The animal centrifuge had an arm length of 1 m and an acceleration range of 1-15 G. Each rabbit was placed inside a cuboid restraint device, which was mounted in the centrifuge arm with the head of the rabbit facing the axis of the centrifuge for +Gz orientation. During the intervals between centrifuge runs, each rabbit was allowed to move freely in the cage.

The +Gz exposure protocol (Figure 1E) was designed according to the national^[23] and international^[24] military standards. The growth rate of +Gz was 1 G/s, the peak value was 4-9 G, the peak duration was 10-45 s, and the interval time was 1 min. The experimental rabbits were exposed to +Gz 3 times a week (every Monday, Wednesday, and Friday).

Harvesting of the Specimens

To monitor new bone formation around the implants, the rabbits were subcutaneously injected with calcein (10 mg/kg body weight) (Sigma Chemical Co., St. Louis, MO, USA) 14 days before being sacrificed and with tetracycline hydrochloride (30 mg/kg body weight) (Sigma Chemical Co., St. Louis, MO, USA) 4 days before being euthanized^[25,26].

The rabbits were sacrificed by an intravenous injection of pentobarbital sodium (Sinopharm Chemical Reagent, Beijing, China). Then, the soft tissues were stripped off and both sides of the jaw were harvested. The left-sided implants and the surrounding bone were fixed in 70% ethanol for micro-CT examination and histological observation. The right-sided implants and the surrounding bone were carefully collected using a Φ 5 mm trephine bur (GC Dental, Tokyo, Japan); afterward, the surrounding 1 mm bone was scraped from the implant and frozen at -80°C until analysis.

Micro-CT Analysis

To evaluate the mass and microarchitecture of the bone surrounding the implants, micro-CT was performed using the Inveon MM system (Siemens, Munich, Germany). Images were acquired with an effective pixel size of 8.99 μm , voltage of 80 kV, current of 500 μA , and exposure time of 1,500 ms during each of the 360 rotational steps. The bone histomorphometric parameters were calculated using the Inveon Research Workplace (Siemens) as

follows: bone volume fraction (BV/TV), trabecular thickness (Tb.Th), trabecular number (Tb.N), and trabecular separation (Tb.Sp) in the area of 1 mm around the middle and lower 2/3rds of the implant.

Fluorescence Double Labeling

After micro-CT analysis, the specimens were dehydrated in an ascending series of ethanol, cleared in chloroform, embedded in methyl methacrylate, sliced into sections of approximately 200 μm along the buccal-lingual axis of the implant by using a rotary diamond saw (SP1600, Leica, Nussloch, Germany), and then ground to a final thickness of approximately 30 μm . The slices were observed under a fluorescence microscope (BX61, Olympus, Tokyo, Japan), and the mineral apposition ratio (MAR, the ratio of the mean vertical distance between the two fluorescence lines and the time interval) at different time points was quantitatively analyzed using Image-Pro Plus (Media Cybernetics, Silver Spring, MD, USA).

Histological Examination

After fluorescence observation, the slices were stained with methylene blue (Sinopharm Chemical Reagent, Beijing, China) and acid magenta (Sinopharm Chemical Reagent, Beijing, China) and observed under a microscope (BX61, Olympus). The bone implant contact (BIC, the percentage of the linear surface of the implant in direct contact with the mineralized bone) was quantitatively analyzed using Image-Pro Plus. BIC was measured as a range covering the mesial and distal sides of the middle and lower 2/3rds of the long axis of the implant, excluding the bottom of the implant.

Real-time Polymerase Chain Reaction (RT-PCR)

Total cellular RNA was extracted from the frozen bone tissue around the implants using the Ultrapure RNA Kit (CoWin Bioscience, Beijing, China) following the manufacturer's instructions. The concentration of RNAs was analyzed by Nanodrop ND-2000 (Thermo, Wilmington, DE, USA) at a wavelength of 260 nm. The purity of RNAs was also determined by the ratio of RNA OD260/OD280. Isolated RNA (2 μg) was reverse-transcribed into cDNA in a reaction mixture containing 4 μL of 5 \times RT buffer, 4 μL of dNTP mixture (2.5 mmol/L), 2 μL of primer mix, and 1 μL of SuperRT (200 U/ μL) in a total volume of 20 μL using the SuperRT One-Step RT-PCR Kit (CoWin Bioscience, Beijing, China). The reaction mixture was incubated at 50 $^{\circ}\text{C}$ for 50 min and at 85 $^{\circ}\text{C}$ for 5 min in a Veriti 96-well Fast Thermal Cycler (Applied Biosystems,

Foster City, CA, USA).

Real-time PCR was performed on the Roche LightCycler 480 PCR system (Roche, Basel, Switzerland) using the Power SYBR green PCR Master Mix (Applied Biosystems, Foster City, CA, USA). Primer sequences (forward and reverse) of the detected genes and the control gene GAPDH (Table 1) were designed according to the published sequences by using Primer Premier 5.0 (Premier Biosoft, Palo Alto, CA, USA) and synthesized by Applygen Technologies Inc (Beijing, China). The PCR amplification reaction mixture (in a final volume of 25 μ L) contained 12.5 μ L of PCR Master Mix, 1 μ L of cDNA, 1 μ L of forward primers, and 1 μ L of reverse primers for the detected genes and GAPDH. PCR conditions used were as follows: pre-denaturation for 10 min at 95 °C, denaturation for 15 s at 95 °C, and annealing for 15 s at 60 °C and extension for 35 s at 72 °C for a total of 40 cycles. Each individual cDNA sample for each gene was assayed in triplicate. A control sample without cDNA was used in each run to exclude genomic DNA contamination. After performing PCR, the Ct values of each sample were collected using MxPro-Mx3005p QPCR Software (Agilent, Santa Clara, CA, USA).

Statistical Evaluation

Statistical evaluation of the data was performed using the SPSS 19.0 software (IBM, Armonk, NY, USA). Mean values and standard deviations were calculated. The differences between the two groups were analyzed using two independent samples *t*-test, and the differences within groups were first analyzed using one-way ANOVA, followed by the Fisher's Least Significant Difference (LSD) tests. Differences were considered statistically significant at $P < 0.05$.

RESULTS

All the rabbits went through the surgery and recovered well. No signs of inflammation were noticed at the surgical sites. The experimental rabbits could endure the predetermined +Gz exposure. Mean body weight and daily food consumption between the control and experimental rabbits were not significantly different during the entire experiment.

Micro-CT Analysis

The images obtained by micro-CT showed that osseointegration was observed in all implants, and the trabecular bone had closely surrounded the implants at 12 weeks (Figure 2A, 2B). BV/TV, Tb.Th, and Tb.N values were increased, and the Tb.Sp value was decreased in both groups as the observation time period increased. In the control group, the changes that occurred from 3 weeks to 5 weeks were more obvious than the changes that occurred from 5 weeks to 12 weeks, and these changes were also more obvious than the changes that occurred from 3 weeks to 5 weeks in the experimental group. BV/TV and Tb.N values were significantly lower, while the Tb.Sp value was significantly higher in the experimental group [(38.80 \pm 5.10)%, (4.79 \pm 0.37)/mm, and (130.03 \pm 17.98) μ m respectively] compared with the control group [(47.85 \pm 5.03)%, (5.40 \pm 0.25)/mm, and (103.31 \pm 11.13) μ m respectively] at 5 weeks (all $P < 0.05$). However, there was no significant difference between the two groups at 3 weeks and 12 weeks (Figure 2C).

Fluorescence Double Labeling

Under a fluorescence microscope, we were able to detect green fluorescence (calcein) near the implant surface and yellow fluorescence

Table 1. Primer sequence of the detected genes

Target gene	Forward primer (5'→3')	Reverse primer (5'→3')
<i>BMP-2</i>	TGAGGATTAGCAGGTCTTT	GCTGGATTGAGGCGTTT
<i>OPN</i>	GCTAAACCCTGACCCATCT	CGTCGGATTATTGGAGT
<i>TGF-β1</i>	AGGACCTGGGCTGGAAGTG	GCGCACGATCATGTTGGA
<i>RANKL</i>	AATGCCCGATTATGTAGGAG	AGATCGAACCATGAACCTTCC
<i>OPG</i>	GATCCAGAACTCTCGTCAG	TGTGCCAAGTGTCTGTGTAG
<i>GAPDH</i>	GGTCGGAGTGAACGGATT	CTCGCTCTGGAAGATGG

Note. *BMP-2*, bone morphogenetic protein-2; *OPN*, osteopontin; *TGF- β 1*, transforming growth factor- β 1; *RANKL*, receptor activator of nuclear factor κ B ligand; *OPG*, osteoprotegerin; *GAPDH*, glyceraldehyde-3-phosphate dehydrogenase.

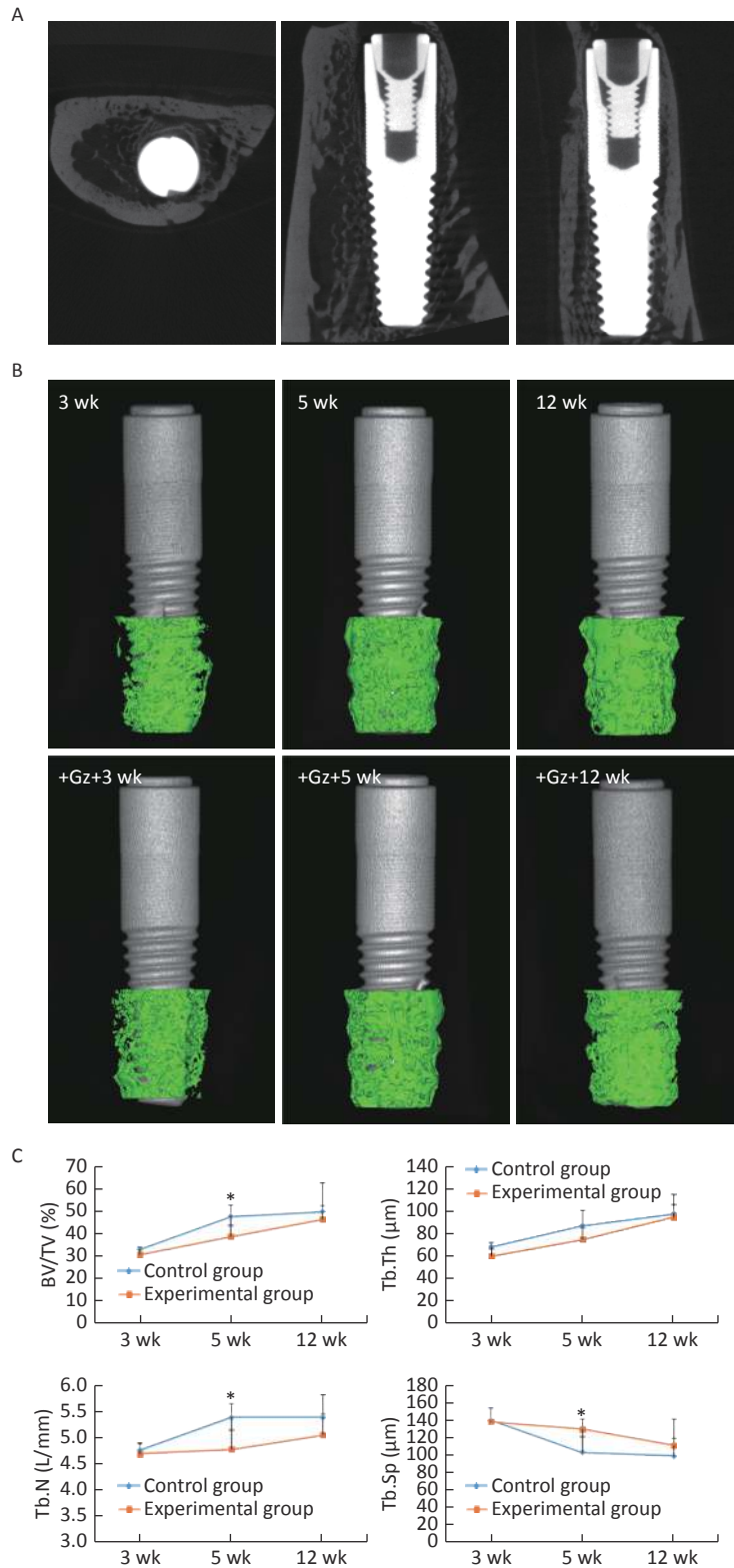


Figure 2. Micro-CT analysis of the implants. (A) Three-dimensional reconstruction of the implant in the experimental group at 12 weeks. (B) Three-dimensional reconstruction of the trabecular bone in the ROI area of the implants in each group. (C) The bone histomorphometric analysis in the ROI area of the implants. * $P < 0.05$ as compared to the control group at the same time point. wk, week.

(tetracycline hydrochloride) further away from the implant surface. The interval between the outside of the green fluorescence and the outside of the yellow fluorescence was the new bone formed during double labeling.

Scattered green and yellow fluorescences were observed in the 3-week control slices, while yellow fluorescence was not very obvious in the 3-week experimental slices. Both linear green and yellow fluorescent ribbons were observed in the 5-week control slices, and the distance between the green ribbon and the yellow ribbon was obvious. The fluorescent ribbons were weak and uneven, and the distance between the green ribbon and the yellow ribbon was narrow in the 5-week experimental group. At 12 weeks after surgery, there was only a small green and yellow fluorescence overlap around

the implants both in the control group and the experimental group (Figure 3A).

MAR in the experimental group at 3 weeks and 5 weeks after surgery [$(1.54 \pm 0.24) \mu\text{m}/\text{d}$ and $(1.66 \pm 0.19) \mu\text{m}/\text{d}$, respectively] was significantly lower than that in the control group [$(1.77 \pm 0.20) \mu\text{m}/\text{d}$ and $(2.07 \pm 0.31) \mu\text{m}/\text{d}$, respectively] (3 weeks $P < 0.05$, 5 weeks $P < 0.01$) (Figure 3B).

Histological Examination

After 3 weeks of the healing period, the newly formed trabecular bone with osteoblasts at the edge was in direct contact with the partial implant surface, and it had spread over the implant surface, towards the host bone (contact osteogenesis). However, there were many inflammatory cells and loose connective tissue in some areas around the

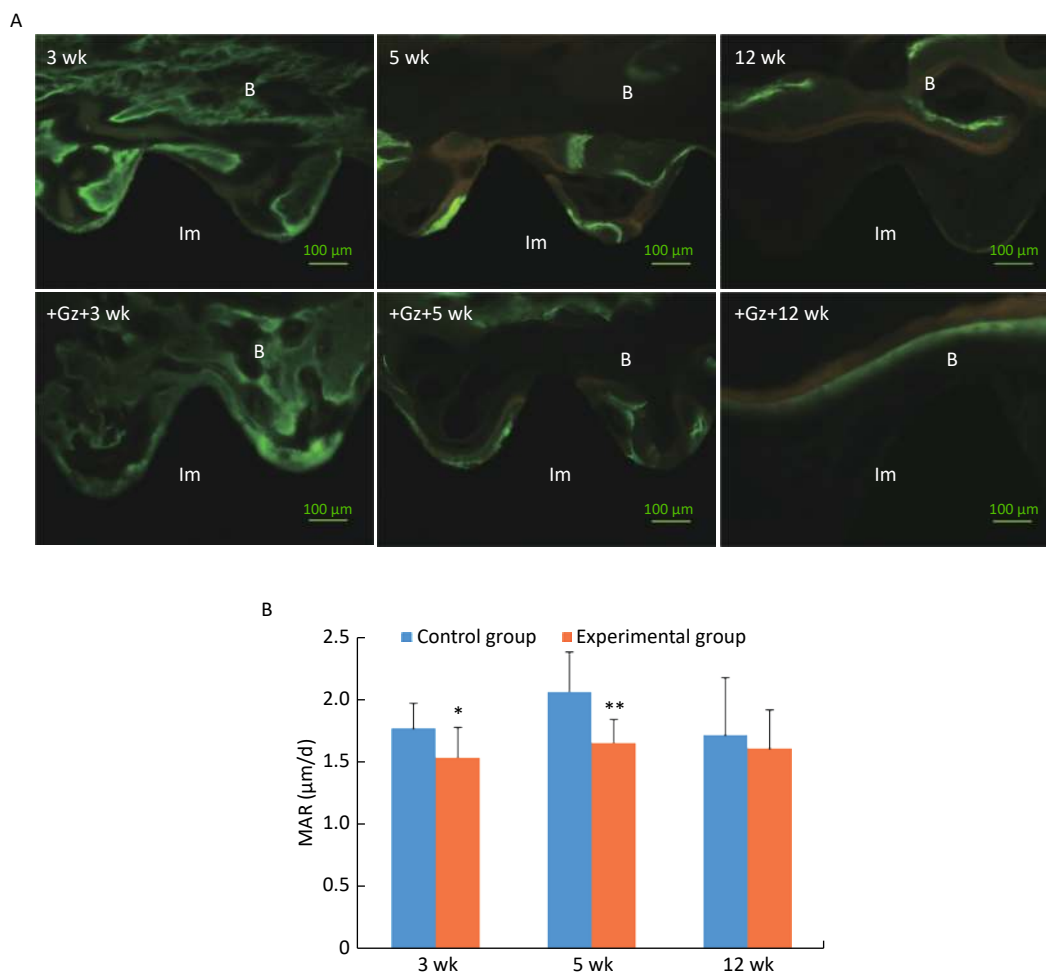


Figure 3. Fluorescence double labeling observation of the implants. (A) Fluorescence microscopic images with the double labeling of calcein and tetracycline hydrochloride in each group (200 \times) (Im: implant, B: bone). (B) Comparison of mineral apposition ratio (MAR) of the implants. Scale bar indicates 100 μm ; * $P < 0.05$, ** $P < 0.01$ as compared to the control group at the same time point. wk, week.

experimental implants. At 5 weeks after surgery, the newly formed peri-implant trabecular bone continued to spread over the implant surface and was connected with the new bone developed from the host bone cavity towards the implant surface (distance osteogenesis). Bone remodeling was active and mature trabecular bone was formed. At 12 weeks after surgery, all implants were surrounded by thick and dense lamellar bone (Figure 4A).

The value of BIC was significantly increased in both groups as the observation time period increased, and it was significantly lower in the experimental group [(40.42 ± 2.85)% and (55.97 ± 5.27)%, respectively] than in the control group [(51.97 ± 6.74)% and (63.74 ± 5.56)%, respectively] at 5 weeks and 12 weeks (both $P < 0.05$) (Figure 4B). Even so, the value of BIC in the experimental group at 12 weeks was up to 55.97%, and it was adequate to ensure implant stability and long-term use^[27,28].

RT-PCR

The mRNA expression levels of bone morphogenetic protein-2 (BMP-2), osteopontin (OPN), transforming growth factor- β 1 (TGF- β 1), receptor activator of nuclear factor κ B ligand (RANKL), and osteoprotegerin (OPG) were highest at 3 weeks after surgery, and then, these levels decreased gradually at 5 weeks and 12 weeks. At 3 weeks after surgery, the mRNA expression levels of BMP-2, OPN, and TGF- β 1 were significantly lower (0.55-, 0.60-, and 0.80-fold, respectively), and the mRNA expression level of RANKL and RANKL/OPG ratio were significantly higher (1.23- and 1.47-fold, respectively) in the experimental group than in the control group (all $P < 0.05$). At 5 weeks after surgery, the mRNA expression levels of TGF- β 1 and OPG were significantly lower (0.77- and 0.75-fold, respectively), and the mRNA expression level of RANKL and

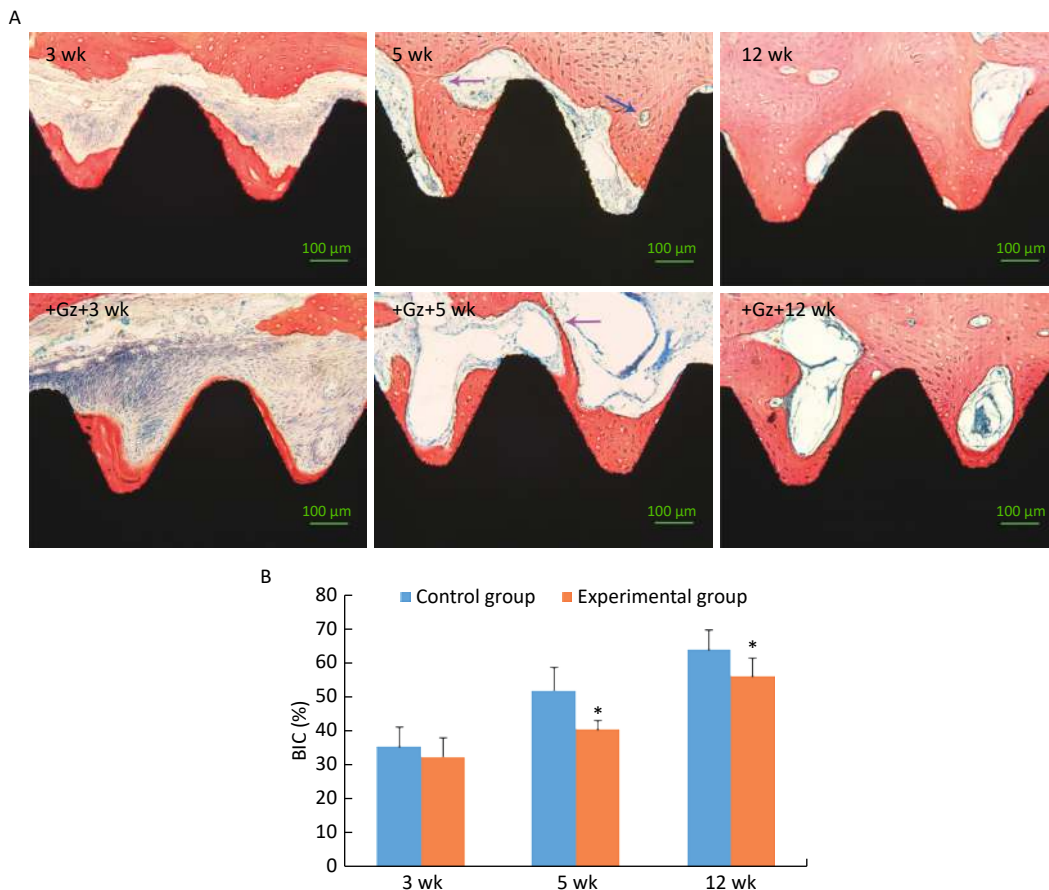


Figure 4. Histological examination of the implants. (A) Histological images of the implant-bone ground slices stained with methylene blue and acid magenta (200 \times). The purple arrow indicates the place where distance osteogenesis and contact osteogenesis were connected. The blue arrow indicates an osteoclast. Scale bar indicates 100 μ m. (B) Comparison of bone-implant contact (BIC) of the implants. * $P < 0.05$ as compared to the control group at the same time point. wk, week.

RANKL/OPG ratio were significantly higher (1.26- and 1.72-fold, respectively) in the experimental group than in the control group (all $P < 0.05$). At 12 weeks after surgery, there was no obvious difference in the mRNA expression levels of the detected genes between the two groups (Figure 5).

In summary, all implants had good osseointegration at 12 weeks. Differences in mRNA expression of osteoblast and osteoclast activity-related cytokines between the two groups were found mainly at 3 weeks and 5 weeks. Differences of the microarchitecture and osseointegration were found mainly at 5 weeks and 12 weeks.

DISCUSSION

In the present study, we found that early exposure to the high +Gz environment after tooth implant surgery can inhibit osseointegration of dental implants by inhibiting osteogenesis of osteoblasts and promoting bone resorption by osteoclasts. This is the first study to assess the effect of high +Gz environment on osseointegration. To elucidate the mechanisms of the effect of high +Gz environment, we further assessed the mRNA expression levels of some cytokines closely related to the function of osteoblasts and osteoclasts by using RT-PCR.

In this study, we used the rabbit incisor immediate implant model taking into account the experimental condition of the animal centrifuge and the anatomical features of the rabbit mandibular structure. Our animal centrifuge can only centrifuge

small animals such as rabbits and rats, but cannot centrifuge large animals like pigs and dogs. *In vivo* studies that use rabbits to evaluate implant osseointegration are usually carried out in the tibia or the femur^[29,30]. However, the stress states of the jaw and the tibia or the femur are different when exposed to +Gz environment. Due to the rabbit's short mouth opening range, it is difficult to extract the teeth and place implants in the rabbit molar area. However, the alveolar bone in the anterior region of the rabbit is thin and a remarkable reduction in the height and width of the alveolar ridge often occurs following tooth extraction^[31,32]. Implant placement immediately after tooth extraction may prevent the occurrence of this atrophy. Indeed, as previously demonstrated by Weber et al.^[33], the rabbit incisor immediate implant model is a feasible and successful *in vivo* model for the investigation of osseointegration.

We choose the middle and lower 2/3^{rds} of the implant as the region of interest (ROI) both in micro-CT observation and histological evaluation because the middle and lower 2/3^{rds} of the implant was more closely contacted by the surrounding alveolar bone after immediate implant placement.

We observed in this study that the values of BV/TV, Tb.Th, Tb.N, and BIC were gradually increased, and the Tb.Sp value was gradually decreased during the observation time period in the two groups. The changes that occurred from 3 weeks to 5 weeks were more obvious than the changes that occurred from 5 weeks to 12 weeks in the control group, indicating that new bone was formed mainly

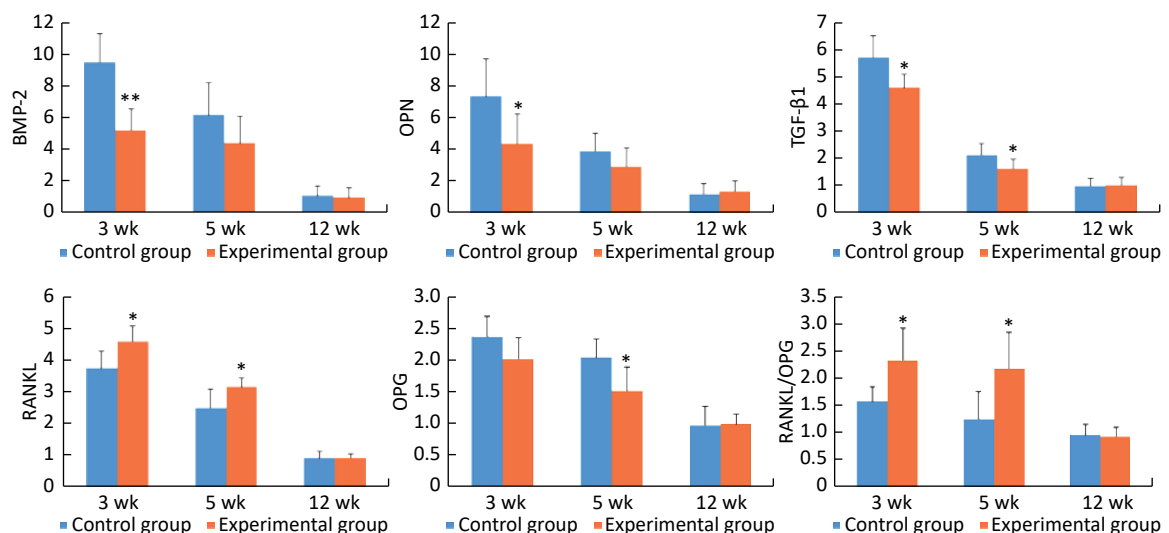


Figure 5. The relative mRNA expression levels of the detected genes in peri-implant bone tissues. * $P < 0.05$, ** $P < 0.01$ as compared to the control group at the same time point. wk, week.

in the first 5 weeks after surgery. After 5 weeks, bone remodeling occupied the first place, mineralization of the new bone tissue was increased, and mature lamellar bone was formed. This process was similar to that described in previous studies^[34-36]. Compared with the values in the control group, the values of BV/TV, Tb.N and BIC in the experimental group were significantly lower and the Tb.Sp value was significantly higher at 5 weeks. MAR in the experimental group was significantly lower than that in the control group both at 3 weeks and 5 weeks. These results indicated that exposure to the +Gz environment may slow down new bone formation and mineralization, and it might have an adverse effect on osseointegration. Nevertheless, both the micro-CT observation and histological evaluation of the specimens in this study showed that initial osseointegration was achieved in all implants after a healing period of 12 weeks. Some experts believe that the value of BIC in a clinically successful implant should be at least 50%^[27,28]. In our study, although the value of BIC in the experimental group was significantly lower than that in the control group at 12 weeks, both these values were above 50%. Good osseointegration was achieved to ensure the stability of the implants and their long-term use. This result indicated that the adverse effect of high +Gz environment on osseointegration was reversible if the exposure time was not very long.

The placement of an implant into a bone activates a wide range of biological reactions, including new bone formation and bone remodeling^[37-39]. Therefore, osseointegration is a complex process involving a number of cytokines.

BMP-2 can promote the transformation of the surrounding mesenchymal stem cells into osteoprogenitors, and it plays an important role in the induction of osteogenesis^[40,41]. OPN is a characteristic marker of osteoblasts in the matrix formation and maturation stage, and it also plays an important role in bone formation and bone remodeling^[42,43]. TGF- β 1 is essential for osteoblastic differentiation of mesenchymal precursors. It can induce the synthesis of BMPs and promote the production of osteoid and extracellular proteins, such as collagen, OPN, and osteonectin^[44]. At 3 weeks, the mRNA expression levels of BMP-2, OPN, and TGF- β 1 in the experimental group were significantly lower than those in the control group. At 5 weeks, the mRNA expression level of TGF- β 1 in the experimental group was still significantly lower than that in the control group. These findings indicated that high +Gz environment may suppress

the osteogenic activity of osteoblasts.

RANKL can bind to the receptor activator of nuclear factor κ B (RANK) on osteoclast precursors, promote osteoclast precursor differentiation, increase osteoclast production, and regulate osteoclast-mediated resorption. OPG can also bind to RANK and block the RANKL/RANK interaction, and thus, it can inhibit osteoclastogenesis and bone resorption^[45]. The balance of RANKL and OPG controls osteoclast activity; therefore, it is usually preferable to evaluate the RANKL/OPG ratio rather than the RANKL and OPG absolute values^[46]. Our study showed that the expression level of RANKL mRNA and RANKL/OPG ratio in the experimental group were significantly higher than those in the control group both at 3 weeks and at 5 weeks, indicating that high +Gz environment can increase the activity of osteoclasts and promote bone resorption.

There were some limitations of the present study. The initial stability of implants is a key factor in osseointegration. Several studies have shown that micro-mobility greater than 150 μ m may affect osseointegration of the implants, resulting in the implants being enwrapped by fibrous tissue^[47-49]. As the implant site was the cancellous bone in the rabbit mandible, the implant torsional moment in our study was 15 N \cdot cm, which is lower than the normal requirement of 30 N \cdot cm^[50]. This may have slightly reduced the initial stability of implants and increased the micro-mobility caused by high +Gz.

CONCLUSIONS

In conclusion, within the limitations of this study, we assessed the effect of high +Gz environment on dental implant osseointegration. We found that early exposure to the high +Gz environment after tooth implant surgery might have an adverse effect on osseointegration, but the effect of short time exposure on osseointegration was reversible. Furthermore, we demonstrated that high +Gz environment may inhibit osteogenesis of osteoblasts by decreasing the mRNA expression levels of BMP-2, OPN, TGF- β 1, and OPG, and it may promote bone resorption by osteoclasts by increasing the mRNA expression level of RANKL and RANKL/OPG ratio. The outcome of this study is of great interest, and it has implications for the application of dental implants in fighter pilots and astronauts. Based on these results, we recommend that fighter pilots need longer recovery time after tooth implantation, and the exact recovery time should be studied further in

future work.

AUTHOR CONTRIBUTIONS

ZHU Xiao Ru and KE Jie designed the study together. ZHU Xiao Ru and DENG Tian Zheng performed the experiments. PANG Jian Liang and LIU Bing analyzed the data. ZHU Xiao Ru wrote the manuscript. KE Jie reviewed the manuscript.

CONFLICTS OF INTEREST

The authors declare no conflict of interest.

Received: February 9, 2019;

Accepted: July 12, 2019

REFERENCES

- Banks RD, Brinkley JW, Allnut R, et al. Human response to acceleration. In: Davis JR, Johnson R, Stepanek J, Fogarty JA (eds). *Fundamentals of aerospace medicine*. 4th ed. Philadelphia: Lippincott Williams & Wilkins, 2008; 83-109.
- Hodkinson PD, Anderton RA, Posselt BN, et al. An overview of space medicine. *Br J Anaesth*, 2017; 119, i143-53.
- Burton RR, Whinney JE. Biodynamics sustained acceleration. In: Dehart LR, Davis RJ (eds). *Fundamentals of aerospace medicine*. 3rd ed. Philadelphia: Lippincott Williams & Wilkins, 2002; 122-53.
- Nishida Y, Maruyama S, Shouji I, et al. Effects and biological limitations of +Gz acceleration on the autonomic functions-related circulation in rats. *J Physiol Sci*, 2016; 66, 447-62.
- Kobayashi A, Tong A, Kikukawa A. Pilot cerebral oxygen status during air-to-air combat maneuvering. *Aviat Space Environ Med*, 2002; 73, 919-24.
- Kaliakin VV, Bukhtiarov IV, Vasilév AI. Study of mineral saturation of lumbar vertebral bones in the course of systemic exposure to +Gz accelerations. *Aviakosm Ekolog Med*, 1996; 30, 9-13.
- Naumann FL, Bennell KL, Wark JD. The effects of +Gz force on the bone mineral density of fighter pilots. *Aviat Space Environ Med*, 2001; 72, 177-81.
- Canciani B, Ruggiu A, Giuliani A, et al. Effects of long time exposure to simulated micro- and hypergravity on skeletal architecture. *J Mech Behav Biomed Mater*, 2015; 51, 1-12.
- Gnyubkin V, Guignandon A, Laroche N, et al. Effects of chronic hypergravity: from adaptive to deleterious responses in growing mouse skeleton. *J Appl Physiol*, 2015; 119, 908-17.
- Martinez DA, Orth MW, Carr KE, et al. Cortical bone responses to 2G hypergravity in growing rats. *Aviat Space Environ Med*, 1998; 69, A17-22.
- Kawao N, Morita H, Obata K, et al. The vestibular system is critical for the changes in muscle and bone induced by hypergravity in mice. *Physiol Rep*, 2016; 4, e12979.
- Huang Y, Dai ZQ, Ling SK, et al. Gravity, a regulation factor in the differentiation of rat bone marrow mesenchymal stem cells. *J Biomed Sci*, 2009; 16, 87.
- Prodanov L, van Loon JJ, te Riet J, et al. Substrate nanotexture and hypergravity through centrifugation enhance initial osteoblastogenesis. *Tissue Eng Part A*, 2013; 19, 114-24.
- Rocca A, Marino A, Rocca V, et al. Barium titanate nanoparticles and hypergravity stimulation improve differentiation of mesenchymal stem cells into osteoblasts. *Int J Nanomedicine*, 2015; 10, 433-45.
- Nose K, Shibamura M. Induction of early response genes by hypergravity in cultured mouse osteoblastic cells (MC3T3-E1). *Exp Cell Res*, 1994; 211, 168-70.
- Fitzgerald J, Hughes-Fulford M. Gravitational loading of a simulated launch alters mRNA expression in osteoblasts. *Exp Cell Res*, 1996; 228, 168-71.
- Gebken J, Lüders B, Notbohm H, et al. Hypergravity stimulates collagen synthesis in human osteoblast-like cells: evidence for the involvement of p44/42 MAP-kinases (ERK 1/2). *J Biochem*, 1999; 126, 676-82.
- Saito M, Soshi S, Fujii K. Effect of hyper- and microgravity on collagen post-translational controls of MC3T3-E1 osteoblasts. *J Bone Miner Res*, 2003; 18, 1695-705.
- Kawashima K, Shibata R, Negishi Y, et al. Stimulative effect of high-level hypergravity on differentiated functions of osteoblast-like cells. *Cell Struct Funct*, 1998; 23, 221-9.
- Furutusu M, Kawashima K, Negishi Y, et al. Bidirectional effects of hypergravity on the cell growth and differentiated functions of osteoblast-like ROS17/2.8 cells. *Biol Pharm Bull*, 2000; 23, 1258-61.
- Morita S, Nakamura H, Kumei Y, et al. Hypergravity stimulates osteoblast phenotype expression: a therapeutic hint for disuse bone atrophy. *Ann N Y Acad Sci*, 2004; 1030, 158-61.
- Haigneré C, Jonas P, Khayat P, et al. Bone height measurements around a dental implant after a 6-month space flight: a case report. *Int J Oral Maxillofac Implants*, 2006; 21, 450-4.
- Centrifuge high G training scheme and evaluation for high performance aircraft pilots. GJB4423-2002. China: The ministry of health of the general logistics department of the people's liberation army, 2002.
- Stupakov GP, Khomenko MN. Selection and special physiological training of flying personnel to high +Gz-maneuverable flights-main concept//Advisory Group for Aerospace Research & Development (AGARD). Current concepts on G-protection research and development. AGARD-LS-202. France: North Atlantic Treaty Organization (NATO), 1995; 3.1-3.15.
- Nkenke E, Kloss F, Wiltfang J, et al. Histomorphometric and fluorescence microscopic analysis of bone remodelling after installation of implants using an osteotome technique. *Clin Oral Implants Res*, 2002; 13, 595-602.
- Tatara AM, Lipner JH, Das R, et al. The role of muscle loading on bone (Re)modeling at the developing enthesis. *PLoS One*, 2014; 9, e97375.
- Lian Z, Guan H, Ivanovski S, et al. Effect of bone to implant contact percentage on bone remodelling surrounding a dental implant. *Int J Oral Maxillofac Surg*, 2010; 39, 690-8.
- Roberts WE. Bone tissue interface. *J Dent Educ*, 1988; 52, 804-9.
- Cordioli G, Majzoub Z, Piattelli A, et al. Removal torque and histomorphometric investigation of 4 different titanium surfaces: an experimental study in the rabbit tibia. *Int J Oral Maxillofac Implants*, 2000; 15, 668-74.
- Giavaresi G, Ambrosio L, Battiston GA, et al. Histomorphometric, ultrastructural and microhardness evaluation of the osseointegration of a nanostructured titanium oxide coating by metal-organic chemical vapour deposition: an in vivo study. *Biomaterials*, 2004; 25, 5583-91.
- Araújo MG, Wennström JL, Lindhe J. Modeling of the buccal and lingual bone walls of fresh extraction sites following implant installation. *Clin Oral Implants Res*, 2006; 17, 606-14.
- Schropp L, Wenzel A, Kostopoulos L, et al. Bone healing and

- soft tissue contour changes following single-tooth extraction: a clinical and radiographic 12-month prospective study. *Int J Periodontics Restorative Dent*, 2003; 23, 313–23.
33. Weber JB, Mayer L, Cenci RA, et al. Effect of three different protocols of low-level laser therapy on thyroid hormone production after dental implant placement in an experimental rabbit model. *Photomed Laser Surg*, 2014; 32, 612–7.
 34. Jayesh RS, Dhinakarsamy V. Osseointegration. *J Pharm Bioallied Sci*, 2015; 7, S226–9.
 35. Parithimarkalaignan S, Padmanabhan TV. Osseointegration: an update. *J Indian Prosthodont Soc*, 2013; 13, 2–6.
 36. Feng SW, Ho KN, Chan YH, et al. Damping factor as a diagnostic parameter for assessment of osseointegration during the dental implant healing process: an experimental study in rabbits. *Ann Biomed Eng*, 2016; 44, 3668–78.
 37. Carinci F, Pezzetti F, Volinia S, et al. Analysis of MG63 osteoblastic-cell response to a new nanoporous implant surface by means of a microarray technology. *Clin Oral Implants Res*, 2004; 15, 180–6.
 38. Kim CS, Sohn SH, Jeon SK, et al. Effect of various implant coatings on biological responses in MG63 using cDNA microarray. *J Oral Rehabil*, 2006; 33, 368–79.
 39. Kojima N, Ozawa S, Miyata Y, et al. High-throughput gene expression analysis in bone healing around titanium implants by DNA microarray. *Clin Oral Implants Res*, 2008; 19, 173–81.
 40. Carpenter RS, Goodrich LR, Frisbie DD, et al. Osteoblastic differentiation of human and equine adult bone marrow-derived mesenchymal stem cells when BMP-2 or BMP-7 homodimer genetic modification is compared to BMP-2/7 heterodimer genetic modification in the presence and absence of dexamethasone. *J Orthop Res*, 2010; 28, 1330–7.
 41. Nohe A, Keating E, Knaus P, et al. Signal transduction of bone morphogenetic protein receptors. *Cell Signal*, 2004; 16, 291–9.
 42. Standal T, Borset M, Sundan A. Role of osteopontin in adhesion, migration, cell survival and bone remodeling. *Exp Oncol*, 2004; 26, 179–84.
 43. Perrien DS, Brown EC, Aronson J, et al. Immunohistochemical study of osteopontin expression during distraction osteogenesis in the rat. *J Histochem Cytochem*, 2002; 50, 567–74.
 44. Lieberman JR, Daluiski A, Einhorn TA. The role of growth factors in the repair of bone. Biology and clinical applications. *J Bone Joint Surg Am*, 2002; 84-A, 1032–44.
 45. Khosla S. Minireview: the OPG/RANKL/RANK system. *Endocrinology*, 2001; 142, 5050–5.
 46. Trouvin AP, Goëb V. Receptor activator of nuclear factor- κ B ligand and osteoprotegerin: maintaining the balance to prevent bone loss. *Clin Interv Aging*, 2010; 5, 345–54.
 47. Trisi P, Berardini M, Falco A, et al. Validation of value of actual micromotion as a direct measure of implant micromobility after healing (secondary implant stability). An in vivo histologic and biomechanical study. *Clin Oral Implants Res*, 2016; 27, 1423–30.
 48. Wazen RM, Currey JA, Guo H, et al. Micromotion-induced strain fields influence early stages of repair at bone-implant interfaces. *Acta Biomater*, 2013; 9, 6663–74.
 49. Winter W, Klein D, Karl M. Micromotion of dental implants: basic mechanical considerations. *J Med Eng*, 2013; 2013, 265412.
 50. Pierrisnard L, Hure G, Barquins M, et al. Two dental implants designed for immediate loading: a finite element analysis. *Int J Oral Maxillofac Implants*, 2002; 17, 353–62.